Title

Graphene-Based Hyperbolic Metamaterial

Permalink

https://escholarship.org/uc/item/6w1862pt

ISBN

9781467353175

Authors

Othman, Mohamed AK
Guclu, Caner
Capolino, Filippo

Publication Date

2013-07-01

DOI

10.1109/aps.2013.6710903

Peer reviewed

Graphene-Based Hyperbolic Metamaterial

Mohamed A. K. Othman, Caner Guclu, and Filippo Capolino
Department of Electrical Engineering and Computer Science
University of California, Irvine
Irvine, CA, USA
f.capolino@uci.edu

Abstract—**We introduce a graphene-based composite multilayer structure that exhibits hyperbolic-like wavevector dispersion at terahertz and mid-infrared frequencies. The multilayer structure comprises graphene sheets separated by dielectric layers. We formulate the effective permittivity tensor of the multilayer using a simple homogenization scheme. In addition, we employ Bloch theory for evaluating the wavevector dispersion for a propagation mode inside the HM, and show that the homogenization scheme is in good agreement with Bloch theory in a very wide spatial spectrum. We report the tunability of transition from elliptic to hyperbolic iso-frequency wavevector dispersion by varying the chemical potential of graphene sheets.**

I. INTRODUCTION

Hyperbolic metamaterials (HMs) are a subcategory of uniaxially anisotropic materials. In general, the isofrequency wavevector dispersion in an uniaxially anisotropic medium can be elliptic for some polarization (extraordinary waves), and under certain conditions it can evolve into a hyperbolic relation which leads to many interesting physical properties [1], [2]. In case of hyperbolic dispersion, ideally, an infinitely wide spatial spectrum of waves can propagate and carry power as opposed to a finite propagating spectrum in common media. However, realistic HMs allow for the propagation of a finite but still very wide spatial spectrum. For this reason, HMs can be employed in novel applications such as enhancing the local density of states [3], super absorbing near-fields at HM surfaces [4], [5], and hyperlensing [6]. In order to gain a physical insight into wave propagation, we represent a HM as an effective medium with a relative effective permittivity tensor $\underline{\varepsilon}_{eff} = \varepsilon_t(\hat{\mathbf{x}}\hat{\mathbf{x}} + \hat{\mathbf{y}}\hat{\mathbf{y}}) + \varepsilon_z\hat{\mathbf{z}}\hat{\mathbf{z}}$ where z is the axis of anisotropy. Hyperbolic dispersion arises when $\varepsilon_t\varepsilon_z < 0$ [7]. A common HM design at optical frequencies is composed of metal-dielectric multilayers with subwavelength thicknesses, that lead to $\varepsilon_t < 0$ and $\varepsilon_z > 0$ (the expressions of ε_t and ε_z can be found in [7]) in a wide frequency band thanks to the metals' negative permittivity [4].

In this paper we propose a graphene-based HM design for terahertz and low mid-infrared frequencies. In our design, graphene sheets play a similar role to metal layers in a metal-dielectric multilayer HM at optical frequencies. Graphene supports plasmonic modes at upper GHz and lower THz range [8], [9] and it can be modeled as a low-loss inductive layer. Moreover, graphene has an extremely subwavelength lattice constant at infrared frequencies, thus spatial dispersion effects are not significant for practical conditions. The tunabilty of

graphene's sheet conductivity via electrostatic and/or magnetostatic bias allows extensive control of the graphene response.
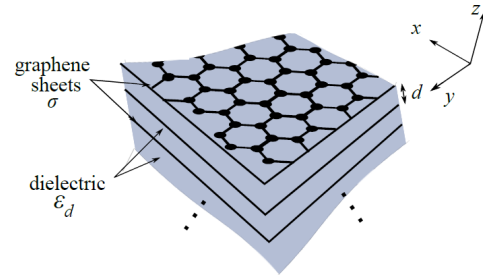

Figure 1. Graphene-based multilayer HM topology, comprises graphene sheets as inductive surfaces stacked with dielectric spacers leading to hyperbolic dispersion at terahertz and mid-infrared frequencies.

II. GRAPHENE-BASED TUNABLE HYPERBOLIC METAMATERIAL

In this paper we investigate the graphene-based HM structure shown in Fig. 1(a) whose unit cell is composed of a graphene sheet and a dielectric layer with relative permittivity ε_d and thickness d. Here we model the graphene sheet using the local isotropic sheet conductivity, $\sigma(\omega, \mu_c) = \sigma' + j\sigma''$, as a function of the chemical potential μ_c (tunable with electrostatic biasing) and frequency, modeled by the Kubo formula [8], assuming a scattering time (Γ^{-1}) of 1 ps, at room temperature. The multilayer metamaterial in Fig. 1 is modeled via effective medium approximation (EMA), with relative permittivity tensor $\underline{\varepsilon}_{eff}$. By averaging the transverse current and electric field (assumed constant over a unit cell), the "transverse" permittivity ε_t is expressed as

$$\varepsilon_t = \varepsilon_t' - j\varepsilon_t'' = \varepsilon_d - j\frac{\sigma(\omega, \mu_c)}{\omega\varepsilon_0 d}. \qquad (1)$$

On the other hand, $\varepsilon_z = \varepsilon_d$ due to the continuity of normal displacement field and the assumption of infinitesimally thin graphene sheets. Straightforwardly, when the graphene sheets are sufficiently inductive, i.e., when $\sigma''(\omega, \mu_c) < -\omega\varepsilon_0\varepsilon_d d$, the effective "transverse" permittivity ε_t becomes negative. This gives rise to hyperbolic wavenumber dispersion for extraordinary (TM^z) wave: $k_z^2/\varepsilon_t + k_z^2/\varepsilon_z = k_0^2$, where k_z

and k_t are the wavenumbers along the z direction and transverse-to-z, respectively. TM^z waves can propagate in the HM with a wide spatial spectrum with $k_t > \sqrt{\varepsilon_d}k_0$, much wider than the propagating spectrum in free space ($k_t < \sqrt{\varepsilon_d}k_0$). Moreover, graphene sheets are highly inductive with a relatively small σ', therefore waves in the graphene-based HM can propagate with limited losses.
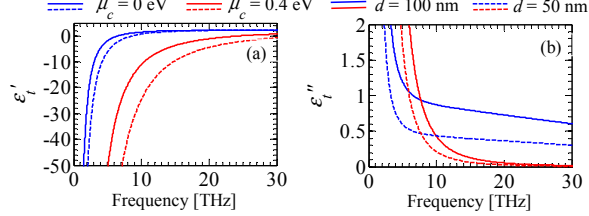

Figure 2. Effective "transverse" relative permittivity (a) real part ε_t' and (b) imaginary part ε_t'' when d = 100 nm (solid lines) and d = 50 nm (dashed lines), for $\mu_c = 0$ eV (blue lines) and $\mu_c = 0.4$ eV (red lines).

In Fig. 2, we report the effective ε_t versus frequency calculated using (1) for various chemical potential values $\mu_c = \{0, 0.4\}$ eV and dielectric thicknesses $d = \{50, 100\}$ nm, assuming $\varepsilon_d = 2.2$. When $\mu_c = 0$ eV, Fig. 2(a) shows that ε_t' exhibits different negative values (necessary for obtaining hyperbolic dispersion) depending on the choice of d, given that the inequality $\sigma''(\omega, \mu_c) < -\omega\varepsilon_0\varepsilon_d d$ is satisfied. ε_t' changes sign at the frequency $\omega = -\sigma''/(\varepsilon_0\varepsilon_d d)$ and becomes positive thereafter. For a given dielectric thickness, the zero-crossing frequency for ε_t' as well as the value of ε_t' can be effectively adjusted by varying μ_c as shown in Fig. 2(a). For example when d = 100 nm, the zero-crossing of ε_t' occurs at ~6.6 THz for $\mu_c = 0$ eV, while it shifts to ~24.5 THz when $\mu_c = 0.4$ eV. As the frequency increases, ε_t' approaches ε_d (not shown here) because graphene conductivity reaches its universal value $\sim \pi e^2/(2h)$ with a negligible reactive part. Note also that ε_t'' exhibits smaller values as the chemical potential is increased (Fig. 2(b)), thus electrostatic biasing also provides tunability of losses. It is important to assess the limits of EMA and characterization of propagating waves inside the graphene multilayer structure. With this aim, we evaluate the wavevector dispersion using the more accurate Bloch theory. Thus in Fig. 3, we use d = 100 nm and report the wavevector dispersion of TM^z waves ($k_z = \beta_z - j\alpha_z$ versus k_t, solutions with α_z representing the waves decaying along the $+ z$ direction) at 10 THz for $\mu_c = \{0, 0.4\}$ eV. In Fig. 3(a) we observe that the wavevector dispersion is elliptic for $\mu_c = 0$ (i.e., $\varepsilon_t' > 0$), and hyperbolic for $\mu_c = 0.4$ eV. (i.e., $\varepsilon_t' < 0$). Recall from Fig. 2 that, when d = 100 nm, the effective permittivity is $\varepsilon_t' = 1.7$
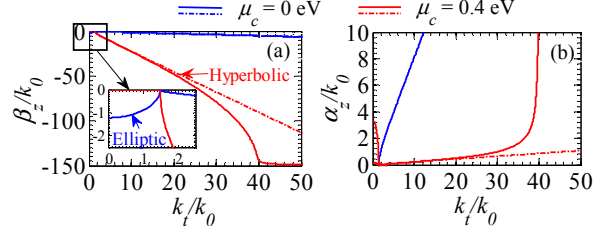

Figure 3. Wavevector dispersion for TM^z waves at 10 THz (a) β_z versus k_t, (b) α_z versus k_t, where $k_z = \beta_z - j\alpha_z$, evaluated via EMA (solid lines) and Bloch theory (dash-dotted lines).

and -11.1 for $\mu_c = 0$ and 0.4 eV, respectively, which proves EMA's effectiveness in interpreting the multilayers transition from elliptic to hyperbolic dispersion. Accordingly, we note that EMA and Bloch theory are in good agreement for small k_t whereas EMA fails to predict the sudden increase of α_z when β_z approaches the Brillouin zone edge denoted by $\beta_z = -\pi/d$ (for a deeper discussion, the reader is referred to [4]). In the hyperbolic dispersion case (with $\mu_c = 0.4$ eV), α_z in Fig. 3(b) is small for a wide spatial spectrum, in which waves can propagate without significant attenuation. In summary, we show that graphene sheets can be used for designing tunable HMs at far and mid-infrared frequencies. The broad spatial spectrum enables the use of the proposed structure to efficiently absorb near fields generated at the HM surface at terahertz frequencies. Graphene-based HM can be utilized for enhancing the scattered power by particles inside or at its surface, and obtaining tunable decay rate of emitters.

REFERENCES

[1] L. B. Felsen and N. Marcuvitz, *Radiation and Scattering of Waves*: Prentice-Hall, NJ, 1973.

[2] D. R. Smith and D. Schurig, "Electromagnetic Wave Propagation in Media with Indefinite Permittivity and Permeability Tensors," *Phys. Rev. Lett.,* vol. 90, p. 077405, 2003.

[3] Z. Jacob, J. Y. Kim, G. Naik, A. Boltasseva, E. Narimanov, and V. Shalaev, "Engineering photonic density of states using metamaterials," *Appl. Phys. B,* vol. 100, pp. 215-218, 2010.

[4] C. Guclu, S. Campione, and F. Capolino, "Hyperbolic metamaterial as super absorber for scattered fields generated at its surface," *Phys. Rev. B,* vol. 86, p. 205130, 2012.

[5] T. Tumkur, L. Gu, J. Kitur, E. Narimanov, and M. Noginov, "Control of absorption with hyperbolic metamaterials," *Appl. Phys. Lett.,* vol. 100, pp. 161103-161103, 2012.

[6] Z. Liu, S. Durant, H. Lee, Y. Pikus, N. Fang, Y. Xiong, C. Sun, and X. Zhang, "Far-field optical superlens," *Nano Lett.,* vol. 7, pp. 403-408, 2007.

[7] O. Kidwai, S. V. Zhukovsky, and J. Sipe, "Effective-medium approach to planar multilayer hyperbolic metamaterials: Strengths and limitations," *Phys. Rev. A,* vol. 85, p. 053842, 2012.

[8] G. W. Hanson, A. B. Yakovlev, and A. Mafi, "Excitation of discrete and continuous spectrum for a surface conductivity model of graphene," *J. Appl. Phys.,* vol. 110, p. 114305, 2011.

[9] M. Tamagnone, J. Gomez-Diaz, J. R. Mosig, and J. Perruisseau-Carrier, "Analysis and design of terahertz antennas based on plasmonic resonant graphene sheets," *J. Appl. Phys.,* vol. 112, p. 114915, 2012.